

# Low-Temperature Sensitive, Compressively Strained InGaAsP Active ( $\lambda = 0.78\text{--}0.85\ \mu\text{m}$ ) Region Diode Lasers

N. Tansu, D. Zhou, and L. J. Mawst

**Abstract**—This letter reports comparative studies between (Al)GaAs versus InGaAsP active region edge-emitting semiconductor lasers for emission wavelength in the IR regime ( $\lambda = 0.78\text{--}0.85\ \mu\text{m}$ ). High characteristic temperature  $T_0$  (200 K) and  $T_1$  (450 K) edge-emitting diode lasers have been demonstrated by using the compressively strained ( $\Delta a/a = 0.6\%$ ) Al-free (InGaAsP) active region with an emission wavelength of  $0.85\ \mu\text{m}$ . The high  $T_0$  and  $T_1$ , a result of low active-layer carrier leakage, will be beneficial for high-temperature and high-power operation. Implementation for InGaAsP-active VCSEL's with compressively strained InGaAsP-active layers and conventional DBR's is also discussed.

**Index Terms**—Diode lasers, epitaxial growth, quantum-well lasers, semiconductor lasers, surface-emitting lasers.

## I. INTRODUCTION

FIBER optics is a popular choice for data link applications due to the higher bit rate and lower cost compared to the conventional copper-based data link systems. VCSEL's at  $\lambda = 0.85\ \mu\text{m}$  are becoming the industry standard for short-distance optical data link applications. At shorter wavelengths, VCSEL's ( $\lambda = 0.76\text{--}0.78\ \mu\text{m}$ ) are needed for applications such as laser printing, optical data storage, and gas spectroscopy. To access this wavelength region, conventional VCSEL's utilize GaAs- or AlGaAs-based active layers. The use of an Al-free InGaAsP-based active region is an attractive alternative to the conventional (Al)GaAs active region for IR VCSEL's. While edge-emitting diode lasers with Al-free active regions have demonstrated performance and reliability surpassing AlGaAs-active devices [1], few studies have been reported on Al-free active VCSEL's in the  $0.78\text{--}0.85\text{-}\mu\text{m}$  wavelength region [2]. Here, we will investigate the properties of compressively strained InGaAsP active-region edge-emitting lasers and the implementation of Al-free active regions into VCSEL's.

To access the  $0.7 < \lambda < 0.80\text{-}\mu\text{m}$  wavelength region, conventional diode lasers utilize AlGaAs quantum-well active regions. However, the high reactivity of aluminum compounds to oxygen leads to bulk degradation, which becomes aggravated as the wavelength becomes shorter (i.e., higher aluminum concentration) [1], [3]. The use of an Al-free InGaAsP active region

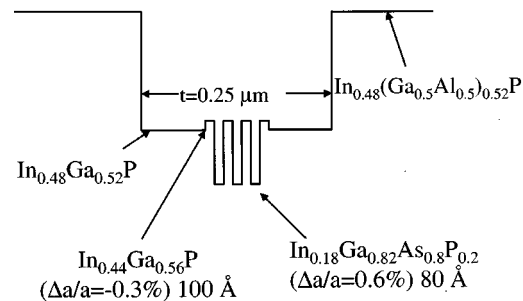


Fig. 1. Schematic energy bandgap diagram for CS-InGaAsP-active region,  $0.85\text{-}\mu\text{m}$  emitting laser structure.

avoids the bulk degradation associated with a large incorporation of oxygen impurities found in AlGaAs-active devices [1], [3]. In addition, the presence of indium in the active region is beneficial in that it inhibits the propagation of dark-line defects [4]. Higher performance is also expected by incorporating compressively strained (CS) quantum-well active regions. Theoretical calculations at  $\lambda = 850\ \text{nm}$  have predicted a lower transparency current density in CS-InGaAsP-active VCSEL's compared to lattice-matched GaAs quantum-well active devices [5]. Furthermore, the use of tensile-strained barriers (InGaP) can provide strain compensation and reduce active region carrier leakage [1]. The fact that Al-free materials are significantly less reactive to  $\text{O}_2$ , compared to AlGaAs materials, also makes them ideal for the fabrication of regrown structures. Index-guided VCSEL's can then be easily fabricated using an etch and regrowth process [6].

## II. EDGE-EMITTING DEVICE STRUCTURES

All the laser structures studied here were grown by low-pressure (50 mbar) metalorganic chemical vapor deposition (LP-MOCVD). TMGa, TMAI, and TMIn are used as the group III sources and  $\text{AsH}_3$  and  $\text{PH}_3$  are used as the group V sources. The Al-free active regions were grown at a temperature of  $700\ ^\circ\text{C}$ , and the GaAs–AlGaAs structures are grown at  $800\ ^\circ\text{C}$ .

The separate confinement heterostructure (SCH),  $0.85\text{-}\mu\text{m}$  emitting Al-free active laser, is shown schematically in Fig. 1. In order to compare device performance between InGaAsP-active and GaAs-active layers, edge emitting lasers were designed and fabricated with identical optical confinement factors ( $\Gamma$ ) and active volumes ( $d$ ). The optical thickness of the InGaP-confinement layers, for the structure shown in Fig. 1, is designed to correspond to the  $\lambda$ -cavity for a VCSEL. However, since the SCH structure is taken directly from the

Manuscript received December 14, 1999; revised February 18, 2000.

The authors are with the Reed Center for Photonics, Department of Electrical Computer Engineering, University of Wisconsin–Madison, Madison, WI 53706-1691 USA.

Publisher Item Identifier S 1041-1135(00)04617-6.

TABLE I  
PERFORMANCE OF InGaAsP-ACTIVE, GaAs-ACTIVE,  
AND BROAD-WAVEGUIDE InGaAsP-ACTIVE  
LASERS FOR 100- $\mu$ m-WIDE  $\times$  1-mm-LONG DEVICES

	InGaAsP	GaAs	BW-InGaAsP
$\lambda$ (nm)	860	850	845
$J_{th}$ (A/cm <sup>2</sup> )	420	350	350
$\eta_d$ (%)	26	26	66
$T_0$ (K)	160	100	212
$T_1$ (K)	410	220	449

VCSEL design (i.e.,  $\lambda$ -cavity), this Al-free laser is not intended to be an optimized edge-emitting laser structure. Tensile ( $\Delta a/a = -0.3\%$ ) strained  $\text{In}_{0.44}\text{Ga}_{0.56}\text{P}$  was used for the barrier layers in order to achieve a higher energy band offset between the barriers and quantum wells [1]. The active region is composed of 3–8-nm-wide QW's of  $\text{In}_{0.18}\text{Ga}_{0.82}\text{As}_{0.8}\text{P}_{0.2}$  with ( $\Delta a/a = 0.6\%$ ) compressive strain. This composition falls outside the miscibility gap for InGaAsP compounds grown at 700 °C [7]. For this structure the optical confinement factor is calculated to be 8.3%.

A comparison structure, consisting of three 8-nm GaAs QW's, was also grown. The GaAs-active structure consists of  $\text{Al}_{0.25}\text{Ga}_{0.75}\text{As}$  and  $\text{Al}_{0.85}\text{Ga}_{0.15}\text{As}$  as confinement/barrier and cladding layers. The thicknesses are chosen to give the same optical confinement factor and active volume as the InGaAsP-active structure.

Broad-area lasers ( $w = 100 \mu\text{m}$ ) are fabricated and compared for performance. The results for as-cleaved devices with cavity lengths of  $L = 1 \text{ mm}$  are shown in Table I. For this value of active layer strain ( $\Delta a/a = 0.6\%$ ), we do not observe a reduction in threshold current density for the Al-free active laser compared with the GaAs-active lasers. This may be a result of poor interface quality between the InGaP and InGaAsP in the active region, or an insufficiently high value of strain. Indium segregation from the InGaP to the InGaAsP is expected to lead to a strained interface [8]. The low value for the external quantum differential efficiency in both structures is simply a result of the large overlap of the optical field with the highly doped cladding layers ( $n, p = 1 \times 10^{18} \text{ cm}^{-3}$ ), which leads to high internal loss  $\alpha_i$ .

The characteristic temperature coefficients of the threshold current density  $T_0$  and external differential quantum efficiency  $T_1$  were measured between 20 °C–60 °C under low duty cycle (1%) pulsed operation. The larger energy bandgap difference between the quantum well active and the cladding layer ( $\Delta E_g = 757 \text{ meV}$  for Al-free active and  $\Delta E_g = 620 \text{ meV}$  for GaAs-active) in the Al-free active structure results in reduced carrier leakage. Thus, the values of  $T_0$  and  $T_1$  for the Al-free active structure are significantly higher compared to the GaAs–AlGaAs laser structure (see Table I). Typical values for  $T_0$  for as-cleaved GaAs single-quantum-well (SQW) lasers are about 100–120 K [9]. The values of  $T_0$  obtained here are comparable with the previously reported  $T_0$  values of GaAs-active [9] and InGaAsP-active ( $T_0 = 160 \text{ K}$ ) diode lasers ( $\lambda = 830 \text{ nm}$ ) [10].

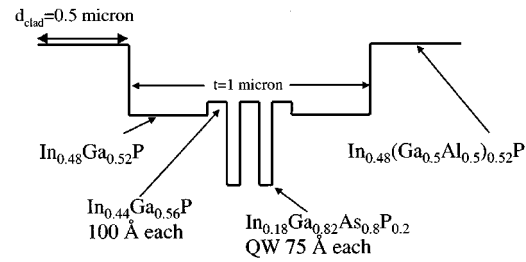


Fig. 2. Schematic energy bandgap diagram of the InGaAsP-active BW laser structure.

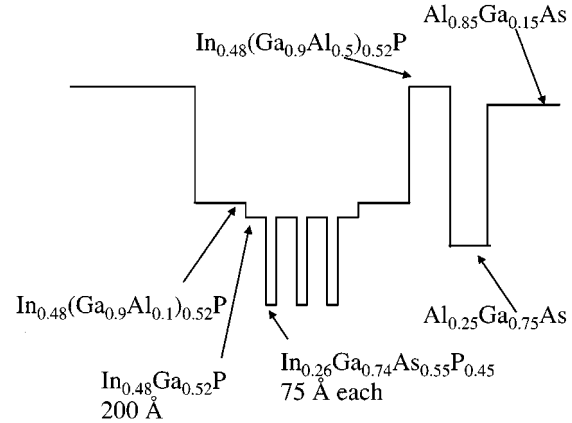


Fig. 3. Schematic energy bandgap diagram of the Al-free active ( $\lambda = 0.78 \mu\text{m}$ ) laser structure with an InGaAsP–AlGaAs interface.

In order to assess the Al-free 0.85- $\mu\text{m}$ -emitting active region for high-power applications, an optimized edge-emitting laser structure was fabricated by using the broad-waveguide (BW) design [8]. The characteristic of BW lasers is that the fundamental transverse mode is designed to have very low loss ( $< 1 \text{ cm}^{-1}$ ), while the second-order transverse mode is suppressed by large radiation losses [10]. For the BW structure shown in Fig. 2, the fundamental mode optical confinement  $\Gamma_o = 2.8\%$  and the effective transverse spot size  $d/\Gamma_o = 0.8 \mu\text{m}$ . The modal radiation loss is calculated to be  $\alpha_o = 0.3 \text{ cm}^{-1}$  and  $\alpha_2 = 112 \text{ cm}^{-1}$  for the fundamental and second-order transverse modes, respectively ( $\Gamma_1 = 0$  for the first-order mode).

Since the InGaP–InGaAsP quantum-well interface is a concern, due to indium segregation from InGaP to InGaAsP, we reduce the number of wells to two. The performance characteristics from the InGaAsP active BW lasers for  $L = 1 \text{ mm}$  and  $w = 100\text{-}\mu\text{m}$  devices are shown also in Table I. Although a low internal loss is observed ( $\alpha_i = 1 \text{ cm}^{-1}$ ), the relatively low internal quantum efficiency ( $\eta_i = 0.72$ ) is believed to reflect the interfacial quality of the InGaP/InGaAsP active region. Previously reported threshold current density ( $J_{th}$ ) and external differential efficiency ( $\eta_d$ ) for ( $\lambda = 830 \text{ nm}$ ) InGaAsP lattice matched-active diode lasers with a BW structure are about 365 A/cm<sup>2</sup> and 77%, respectively [10]. The threshold current density of our GaAs-active lasers is comparable with the previously published results [9]. The high values of  $T_0$  and  $T_1$ , together with the large transverse spot size, is beneficial for high-temperature/high-output power edge-emitter operation. The reduced carrier leakage (high  $T_0$  and  $T_1$ ) is also beneficial for realizing high-temperature and high-power VCSEL operation [11].

### III. IMPLEMENTATION OF THE InGaAsP-ACTIVE INTO VCSEL'S

Al-free active region VCSEL's with conventional AlGaAs-AlAs distributed Bragg reflectors (DBR's) contain an (Al)InGaP-AlGaAs interface between the cavity region and the top p-type DBR, which is susceptible to In segregation [12], [13]. Studies on the InGaIP-AlGaAs interface have been done extensively for visible VCSEL's [13]. The use of an AlAsP transitional layer to continuously grade the group V composition was found to improve the AlGaInP-AlGaAs interface [13].

To study this interface, edge-emitting ( $\lambda = 0.78 \mu\text{m}$ ) Al-free active laser structures were fabricated, as shown in Fig. 3, which contain the AlGaInP-AlGaAs interface representing the top DBR of the VCSEL. A growth pause ( $\sim 1$  min) and temperature ramp ( $T = 700 \text{ }^\circ\text{C}$ – $750 \text{ }^\circ\text{C}$ ) between the AlGaInP and the AlGaAs (top DBR) resulted in significant indium carryover and subsequent high-threshold current densities ( $> 1 \text{ kA/cm}^2$ ). Highest performance was achieved by performing the growth of the Al-free cavity and AlGaAs-based p-DBR at the same temperature ( $T_g = 700 \text{ }^\circ\text{C}$ ), with minimal growth pause and without the use of an interface transitional layer.

For this case, the threshold current density of the lasers is comparable to that of similar laser structures without the AlInGaP-AlGaAs interface ( $J_{\text{th}} = 470 \text{ A/cm}^2$ ,  $L = 1 \text{ mm}$ ).

### IV. CONCLUSION

Compressively strained InGaAsP active ( $\lambda = 850 \text{ nm}$ ) edge-emitting lasers, with tensile-strained InGaP as barriers, exhibit high  $T_o$  (200 K) and  $T_1$  (450 K), which is beneficial for high-power and high-temperature operation. The high value of  $T_o$  and  $T_1$  can be attributed to the larger bandgap difference between the quantum well and the cladding layers for InGaAsP-active lasers compared the the GaAs-active lasers. Further optimization is required to improve the InGaP-InGaAsP quantum well interface to fully utilize the benefits of compressive strain. To implement the InGaAsP-active into VCSEL's, Al-free active cavity and AlGaAs-based p-DBR should be grown at the same growth

temperature (to minimize the pause time). By minimizing the growth pause for the InGa(Al)P-AlGaAs interface, indium carryover is minimized.

### REFERENCES

- [1] L. J. Mawst, S. Rusli, A. Al-Muhanna, and J. K. Wade, "Short-wavelength ( $0.7 \mu\text{m} < \lambda < 0.78 \mu\text{m}$ ) high-power InGaAsP-active diode lasers," *IEEE J. Select. Topics Quantum Electron.*, vol. 5, pp. 785–791, 1999.
- [2] R. P. Schneider and M. Hagerott-Crawford, "GaInAsP-AlGaInP-based near-IR (780 nm) vertical-cavity surface-emitting lasers," *Electron. Lett.*, vol. 31, pp. 554–556, 1995.
- [3] J. S. Roberts, J. P. R. David, L. Smith, and P. L. Tihanyi, "The influence of trimethylindium impurities on the performance of InAlGaAs single quantum well lasers," *J. Crystal Growth*, vol. 195, pp. 668–675, 1998.
- [4] S. L. Yellen, A. H. Shepard, R. J. Dalby, J. A. Baumann, H. B. Serreze, T. S. Guido, R. Soltz, K. J. Bystrom, C. M. Harding, and R. G. Waters, "Reliability of GaAs-based semiconductor diode lasers: 0.6–1.1  $\mu\text{m}$ ," *IEEE J. Quantum Electron.*, vol. 29, pp. 2058–2067, 1993.
- [5] T. E. Sale, C. Amamo, Y. Ohiso, and T. Kurokawa, "Using strained lasers ( $\text{Al}_x\text{Ga}_{1-x}$ )<sub>y</sub>  $\text{In}_{1-y}\text{As}_z\text{P}_{1-z}$  system materials to improve the performance of 850 nm surface- and edge-emitting lasers," *Appl. Phys. Lett.*, vol. 71, pp. 1002–1004, 1997.
- [6] D. Zhou and L. J. Mawst, "S-ARROW VCSELs," in *LEOS'99*, San Francisco, CA, Nov. 1999, pp. 393–394.
- [7] G. B. Stringfellow, *Organometallic Vapor-Phase Epitaxy*, 1st ed. San Diego, CA: Academic, 1989.
- [8] A. Al-Muhanna, L. J. Mawst, D. Botez, D. Z. Garbuzov, R. U. Martinelli, and J. Connolly, "High-power ( $>10 \text{ W}$ ) continuous-wave operation from 100- $\mu\text{m}$ -aperture 0.97- $\mu\text{m}$ -emitting Al-free diode lasers," *Appl. Phys. Lett.*, vol. 73, pp. 1182–1184, 1998.
- [9] K. Shigihara, Y. Nagai, S. Karakida, A. Takami, Y. Kokubo, H. Matsumura, and S. Kakimoto, "High-power operation of broad-area laser diodes with GaAs and AlGaAs single quantum wells for Nd:YAG laser pumping," *IEEE J. Quantum Electron.*, vol. 27, pp. 1537–1543, 1991.
- [10] J. K. Wade, L. J. Mawst, D. Botez, M. Jansen, F. Fang, and R. F. Nabiev, "High continuous wave power, 0.8  $\mu\text{m}$ -band, Al-free active-region diode lasers," *Appl. Phys. Lett.*, vol. 70, pp. 149–151, 1997.
- [11] P. Schnitzer, M. Grabherr, R. Jäger, F. Mederer, R. Michalzik, D. Wiedenmann, and K. J. Ebeling, "GaAs VCSEL's at  $\lambda = 780$  and 835 nm for short-distance 2.5-Gb/s plastic optical fiber data links," *IEEE Photon. Technol. Lett.*, vol. 11, pp. 767–769, July 1999.
- [12] F. Bugge, J. Sebastian, A. Knauer, G. Beister, I. Rechenberg, K. Vogel, G. Erbert, and M. Weyers, "Growth of GaInP/AlGaAs/GaAs structures for high power laser diodes," in *Workshop Booklet, 7th EW MOVPE VII*, Berlin, Germany, 1997.
- [13] R. P. Schneider, "Epitaxial design and performance of AlGaInP red (650–690 nm) VCSELs," in *Current Trends in Vertical Cavity Surface Emitting Lasers*. Singapore: World Scientific, 1995.